MICROWAVE GASEOUS DISCHARGE IN THE
NON-UNIFORM FIELD REGION

by

Lawrence Gould

Submitted in Partial Fulfillment of the
Requirements for the Degree of
Bachelor of Science

at the

Massachusetts Institute of Technology
(1950)

Signature of Author. Signature redacted ....

Department of Physics, September 1, 1950

Certified by....... Signature redacted ....

Thesis Supervisor

TABLE OF CONTENTS

ABSTRACT.....i

ACKNOWLEDGMENT.....ii

INTRODUCTION.....1

BREAKDOWN THEORY.....2

BREAKDOWN IN UNIFORM FIELDS.....4

BREAKDOWN IN NON-UNIFORM FIELDS.....5

VERIFICATION OF THE UNIVERSAL BREAKDOWN CURVE FOR HYDROGEN.....11

EXPERIMENTAL PROCEDURE.....14

RESULTS.....18

REFERENCES.....23

ABSTRACT

The solution of the characteristic breakdown equation, with the proper boundary conditions imposed, leads to a method of calculating an effective diffusion length, Λ_e , for the case of non-uniform fields. Λ_e may be regarded as expressing an equivalent parallel plate separation to give the same breakdown field as that of the actual cavity. This correction is used to obtain values of the ionization coefficients from the breakdown data. The object of this thesis is to prove experimentally that for breakdown in hydrogen the curve of ζ vs. E_e/p is a universal curve, being valid in the uniform and non-uniform field region. Breakdown data is obtained for cylindrical cavities whose ratios of radius to length are as low as 0.5.

ACKNOWLEDGMENT

The author wishes to acknowledge the valuable assistance and encouragement given by his thesis supervisor, Professor S.C.Brown. Sincere appreciation is extended to all the members of the Gas Discharge Group and especially to Mr. K. Persson for his advice on the theory and to Mr. J.J.McCarthy for his help with the experimental technique. The author wishes to thank the Physics Department and the Research Laboratory of Electronics for providing the facilities for the research.

INTRODUCTION

The Townsend theory for breakdown of a low pressure gas under the action of a d.c. electric field postulates two sources of electrons. Most of the electrons are generated in the volume of the gas through ionization by collision. The original source of electrons at the cathode results from secondary emission caused by positive ion or photon bombardment. Prediction of the breakdown voltage requires numerical data on the efficiency of these processes. Thus attempts to determine ionization coefficients from breakdown data have been complicated by the operation of two electron generation processes.

In a high frequency gas discharge breakdown, the primary ionization due to the electron motion is the only production phenomenon which controls the breakdown; the electrons formed at the walls or in the gas by secondary emission have a negligible effect. It is therefore possible to predict the electric field for breakdown from a knowledge of the ionization coefficient only, or to measure the ionization coefficient from a breakdown experiment.

A theory has been developed for the breakdown criterion in TM_{010}-mode cylindrical cavities. The object of the present experiment is primarily to extend the range of the experimental data beyond the region where the cavity height is small compared to its diameter. This generalization removes the assumption that the cavity approximates the conditions of infinite parallel plates. The following theory has been developed by Herlin and Brown (1,2).

BREAKDOWN THEORY

The breakdown condition is developed for a region in a resonant cavity bounded by walls which absorb electrons. A radioactive source near the discharge cavity provides a small amount of ionization in the cavity. The microwave field in the cavity is gradually increased until the gas suddenly begins to glow, becomes conducting, and the field drops to a much lower value. The field necessary to produce this phenomenon is called the breakdown field.

From the principle of balancing the generation of electrons through ionization by collision against the loss of electrons through diffusion, the differential equation and and boundary conditions which lead to the breakdown field strength can be obtained (1). The resulting differential equation is

$$\nabla^2 \psi + \zeta E^2 \psi = 0 \qquad (1)$$

where the electron diffusion current density potential ψ is given by $\psi = Dn$, and ζ is the high frequency ionization coefficient defined by $\zeta = \nu/DE^2$. The quantity n is the electron density function, D is the electronic diffusion coefficient, ν is the net production rate of electrons per electron, and E is the r.m.s. value of the electric field intensity.

The boundary condition on ψ is obtained by setting the diffusion current approaching the wall equal to the random current collected by the wall. It can be shown that the density of the electrons will go to zero at a distance of the order of a mean free path beyond the wall (3). However, because diffusion theory is valid only when the mean free path is small compared to the dimensions of the discharge tube, it is sufficiently accurate to apply the condition that the electron density, and therefore ψ, vanish at the walls.

The ionization coefficient is a function of E/p and $p\lambda$, where E/p expresses the energy gained by an electron per collision at zero frequency, and $p\lambda$ expresses the ratio of the collision frequency of the electrons to the frequency of the applied high frequency field. The quantity p is the pressure and λ is the free-space wave length of the electric field. The electric field appears explicitly in Eq. (1) because it varies with position in the cavity. On the other hand, $p\lambda$ is constant throughout the cavity. The electric field is expressed in the form $E=E_o f(x,y,z)$, where E_o is the maximum value of the field and f is a geometrical factor obtained from a solution of Maxwell's equations for the field distribution within the cavity as an electromagnetic boundary value problem. The value of f is unity at the maximum field point. The magnitude of excitation in the cavity is expressed by E_o, and the relative field distribution through the cavity is independent of the excitation. The boundary value problem of finding a non-zero solution to Eq. (1), with the boundary condition that ψ be zero on the cavity walls, leads to a characteristic value of E_o, which is the breakdown field at the maximum field point.

BREAKDOWN IN UNIFORM FIELDS

If the end plate separation is small compared to the diameter of the region where the field is substantially uniform, in the vicinity of the center of the cavity, then these cavities approximate the conditions of infinite parallel plates with a uniform electric field. Under such conditions, the solution of Eq. (1) is

$$\psi = A \sin (z/\Lambda) \tag{2}$$

where $\Lambda = L/\pi$, L is the plate separation distance, z is the distance from one plate to an arbitrary point in the cavity, and A is a constant. Λ is also known as the diffusion length. The breakdown condition is

$$\zeta = 1/\Lambda^2 E^2 \tag{3}$$

The electric field for breakdown may be measured as a function of pressure, frequency, and plate separation. From this data the ionization coefficient ζ may be computed.

BREAKDOWN IN NON-UNIFORM FIELDS

If the end plate separation cannot be neglected compared to the diameter of the cavity, then the electric field in the cavity can no longer be considered uniform. Its variation with respect to the distance from the center of the cavity must be taken into account. The solution of the characteristic value of Eq. (1) becomes considerably more difficult.

Integration of Eq. (1) is simplified by the use of the approximation employed by Herlin and Brown (1,2).

$$\zeta = \zeta_0 \left(\frac{E}{E_0}\right)^{\beta-2} = \left(\frac{1}{E_0 \Lambda_a}\right)^2 \left(\frac{E}{E_0}\right)^{\beta-2} \qquad (4)$$

where ζ_0 is the value of the ionization coefficient at the maximum field point, Λ_a is introduced for mathematical convenience and has the units of reciprocal length. The quantity $\beta - 2$ is obtained as the slope of the ζ vs. E/p plot on a logarithmic scale at the point E_0/p. This approximation gives accurate results because it is correct where the ionization is high, and is inaccurate only where the ionization is low and therefore has little effect on the solution of the equation.

From the solution of Maxwell's equation the electric field in the TM_{010}-mode cylindrical cavity, shown in Fig. 1, is found to be given by the expression,

$$E = E_0 \, J_0(2.405 \, r/R). \qquad (5)$$

R is the radius of the cavity and J_0 is the Bessel function of order zero.

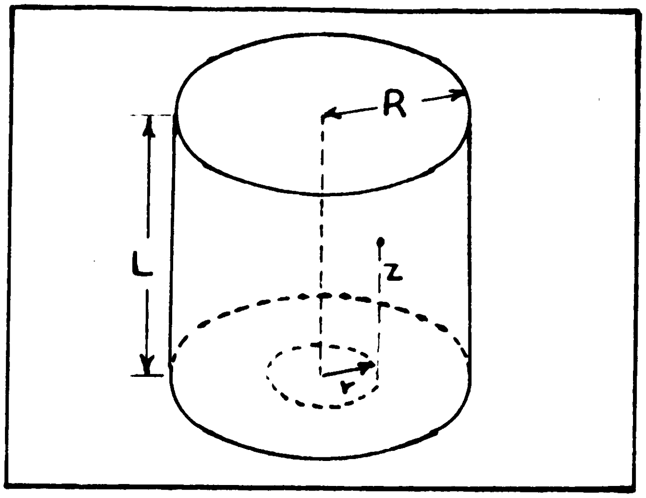

Fig. 1. Cylindrical cavity, showing dimensions and coordinates.

Since the electric field depends on the radical component only, the differential equation, Eq. (1), may be separated. Separation results in

$$\psi = A \sin(\pi z/L)\,\varphi(r) \tag{6}$$

where A is a constant, L is the length of the cylindrical cavity, z is the axial coordinate, and $\varphi(r)$ is determined from the differential equation

$$\frac{1}{r}\frac{d}{dr}\left(r\frac{d\varphi}{dr}\right) + \left[\xi E^2 - (\pi/L)^2\right]\varphi = 0 \tag{7}$$

The approximation of Eq. (4) and the electric field of Eq. (5) substituted into Eq. (7) lead to the equation

$$\frac{1}{r}\frac{d}{dr}\left(r\frac{d\varphi}{dr}\right) + \left[\frac{1}{\Lambda_e^2} J_0^\beta(2.405\,r/R) - (\pi/L)^2\right]\varphi = 0 \tag{8}$$

It is difficult to find an analytic solution to this equation. A good approximation is to express the Bessel function as the first two terms of its power series. This approximation is also valid where the ionization is high and fails only where it low. Equation (8) then becomes

$$\frac{1}{r}\frac{d}{dr}\left(r\frac{d\varphi}{dr}\right) + \left[\frac{1}{\Lambda_e^2}\left(1-\frac{r^2}{b^2}\right) - (\pi/L)^2\right]\varphi = 0 \tag{9}$$

where

$$b = 0.831\, R/g^{1/2} \tag{10}$$

is the radius at which the ionization goes to zero under the above assumptions.

The ionization function in Eq. (9) is negative where $r > b$, which is not physically possible. Accordingly, the ionization is set equal to zero from $r = b$ to $r = R$. Equation (9) is used in the range $0 \leq r \leq b$ and in the range $b \leq r \leq R$ the equation

$$\frac{1}{r}\frac{d}{dr}\left(r\frac{d\varphi}{dr}\right) - \left(\pi/L\right)^2 \varphi = 0 \tag{11}$$

is applied. The ionization function employed here is compared with the actual ionization function in Fig. 2. They are identical in the vicinity of $r = 0$, where the ionization is high. The error in the approximation becomes positive as r increases, and negative as it approaches the radius b. Beyond $r = b$, the ionization drops rapidly to zero and is approximated by the value zero. The boundary condition on φ is that it be zero at $r = R$ and that its derivative and value match at $r = b$.

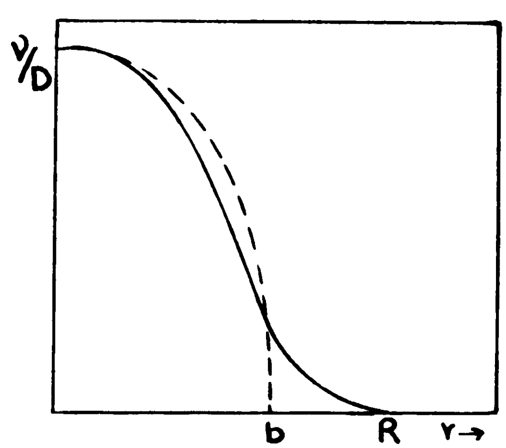

Fig. 2. Comparison of actual ionization function (solid curve) with its approximation (dotted curve).

The solution of Eq. (9) is

$$\varphi = \exp\left(-\frac{\sigma x^2}{2}\right) M\left(\frac{2\sigma-1}{4\sigma}, 1, \sigma x^2\right) \qquad (12)$$

where

$$\sigma = 1/\Lambda_e b\left(1 - \Lambda_e^2 \pi^2/L^2\right)$$

$$x = \left[1 - \pi^2 \Lambda_e^2/L^2\right]^{1/2} r/\Lambda_e$$

and M is the confluent hypergeometric function (4). The second solution is omitted because it has a singularity at the origin. The solution of Eq. (11) is

$$\varphi = i H_0^{(1)}(i\pi r/L) - K J_0(i\pi r/L) \qquad (13)$$

where K is a constant of integration. It is chosen to make φ equal to zero at the point $r = R$, and it is thus a function of R/L. For values of R/L greater than 0.5, the Bessel term may be neglected (2). The range below 0.5 may be computed if the Bessel term is retained. The numerical computations were performed only for $R/L > 0.5$ so that the results here are applicable to cavities whose heights are smaller than their diameter. This increase in the coverage of the range of R/L is a substantial gain over the coverage of the parallel plate treatment, for which R/L should be greater than 15.

The matching condition at $r = b$ may be satisfied by making the ratio φ'/φ equal on both sides of the matching point. φ' is the derivative of φ with respect to r. The resulting equation is a transcendental equation for the breakdown field:

$$\frac{x_0 H_1^{(1)}(i x_0)}{i H_0^{(1)}(i x_0)} = y_0 \left[\frac{2\sigma-1}{2\sigma}\,\frac{M\left(\frac{6\sigma-1}{4\sigma}, 2, y_0\right)}{M\left(\frac{2\sigma-1}{4\sigma}, 1, y_0\right)} - 1\right] \qquad (14)$$

where

$$x_0 = \pi b/L$$

and

$$y_0 = b/\Lambda_e$$

Eq. (14) may be solved for b/Λ_e as a function of L/Λ_e. The results are most conveniently represented by expressing $(\Lambda_e/\Lambda)^2$ as a function of b/L. This plot is shown in Fig. 3.

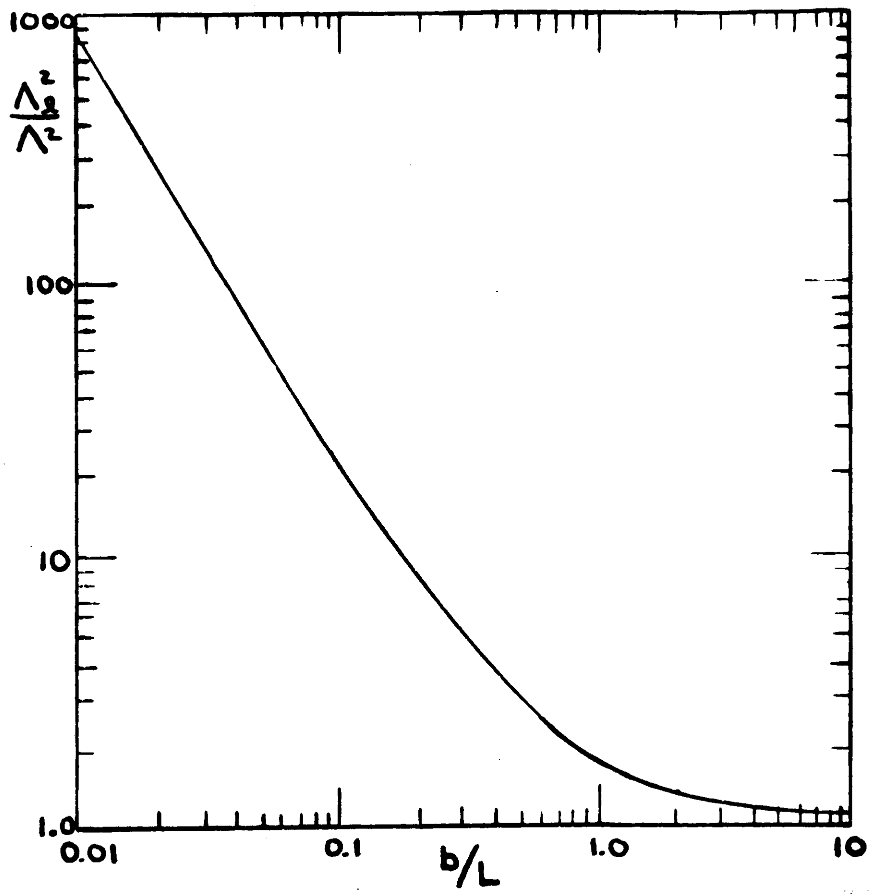

Fig. 3. Solution of the transcendental breakdown equation, Eq. (14).

For the case of a uniform field, the characteristic diffusion length is $\Lambda = L/\pi$. Λ_e may be considered as an effective diffusion length or the equivalent infinite parallel plate separation which will give the same breakdown field as that of the actual cavity. Therefore, at large b/L the conditions of a uniform field prevail and Λ is equal to Λ_e, so that the ordinate of Fig. 3 approaches unity. If the tube is long or the slope of the ionization coefficient curve is large, b/L is small and a larger value of Λ_e, and therefore electric field, is required for breakdown, relative to what would be required with a uniform field.

VERIFICATION OF THE UNIVERSAL BREAKDOWN CURVE FOR HYDROGEN

From the uniform field data for hydrogen a plot of ζ as a function of E_e/p can be obtained. E_e is the effective field defined by the following relation (5)

$$E_e^2 = E^2\left[\frac{\nu_c^2}{\nu_c^2 + w^2}\right] \tag{15}$$

where E is the r.m.s. value of the applied field, ν_c is the collision frequency, and w is the radian frequency of the field, E_e is the effective field which would produce the same energy transfer at zero frequency. The collision frequency as a function of pressure is known from experiment. It is found that for various diffusion lengths the same curve is obtained. It is assumed that ζ as a function of E_e/p is a universal curve and the object of this thesis is to prove experimentally that the curve is also valid in the non-uniform field region. The results obtained in the preceeding sections are used to extend the range of experimental values of the ionization coefficient from experimental data in longer cavities than are permitted by the uniform field theory. From this result, the validity of the universal curve in the non-uniform field region can be tested.

The following procedure is utilized: From the plot of $\left(\frac{1}{E\Lambda}\right)^2$ as a function of E/p, the slope of the constant $p\lambda$ curves are plotted as a function of E/p. The ordinate $\left(\frac{1}{E\Lambda}\right)^2$ would be the high frequency coefficient if the experiment were performed between infinite parallel plates. If this assumption is made, the slope of the constant $p\lambda$ curves would be the β contained in Eq. (4). As a first approximation this value of β is used to find the effective diffusion length from Fig. 3. Thus, a second approximation to the ionization coefficient curves is obtained. The process is repeated until no further correction is indicated. In order for the theory to be valid, any correction to the ionization curves after the first correction is made should be only a second order effect. This method has also been used satisfactorily in the case of electron diffusion in a spherical cavity by MacDonald and Brown (6).

Another method of verifying the universal curve of ζ vs. E_e/p in the non-uniform field region has been suggested by Karl-Berger Persson. A curve of ν/D as a function of the radius of a given cavity in the non-uniform field region may be obtained from the above curve and the fact that $\nu/D = \zeta E^2$. The curve will appear similar to the one in Fig. 2. If this curve can be expressed as an analytic function of the radius, it may be inserted in Eq. (7). The procedure is to retain an arbitrary constant in the expression of ν/D as a function of the radius and to determine this constant from solving the characteristic breakdown equation. If this constant agrees with the actual value, then it may be assumed that the curve of ζ as a function of E_e/p is valid in the non-uniform field region. Although the above method appears reasonable in theory, it is very difficult to perform in practice. The obstacle encountered is that the differential equation obtained by inserting the function ν/D in Eq. (7) cannot as yet be solved by known methods of integration. However, it may be possible that an approximation similar to the one discussed on page 7 can be made such that the differential equation becomes integrable. This method of approach will be attempted after the complete set of experimental data is obtained.

EXPERIMENTAL PROCEDURE

A block diagram of the apparatus used in the experiment is shown in the following figure.

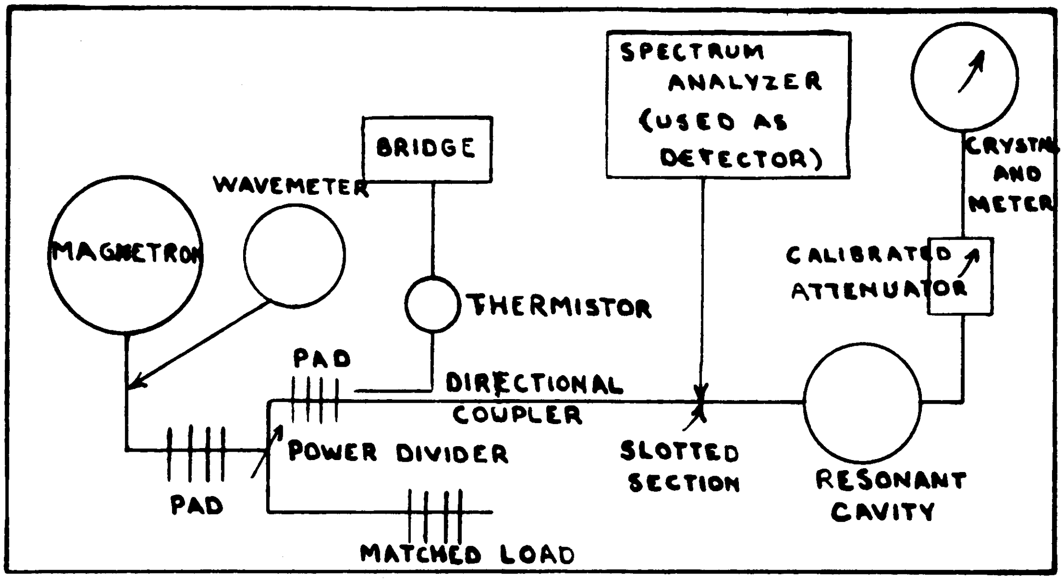

A continuous-wave tunable magnetron in the 10 cm. wave length region supplies microwave power into a coaxial line connecting to the measurement equipment. In order to prevent leakage of the magnetron power from introducing an interfering signal in the measurements, a brass shield, enclosing the magnetron, is used. The stability of the input power is improved by employing a regulated voltage supply.

A cavity wavemeter determines the frequency of the magnetron power. The power incident on the cavity is varied by a power divider. A directional coupler provides a known fraction of the incident power to a thermistor element, whose resistance, measured by a sensitive bridge, indicates power incident on the cavity. The slotted section is a standing wave detector which determines the field in the coaxial transmission line as a function of distance. The power picked up by the probe in the slotted section is transmitted through an adjustable, calibrated attenuator to the input terminals of the spectrum analyzer. The standing wave ratio in decibels can be determined directly from the attenuator readings.

The cavities are designed so that they resonate in the TM_{010} -mode in the 10 cm. wave length region, and are coupled to the coaxial transmission line by a coupling loop. A second coupling loop provides a transmitted signal to a cut-off attenuator terminated in a crystal rectifier and micro-ammeter. A description of the equipment and the method of calibrating and adjusting it is given in reference (8).

The cavities were made of oxygen-free high conductivity copper and all joints were hard soldered. The coupling loops were made of copper, Kovar, and glass. The cavity was connected through Kovar to an all glass system including a three stage oil diffusion pump and a liquid nitrogen trap. The vacuum was measured by an ionization guage. In order to obtain as high a degree of purity as possible, the cavity and ionization guage were baked at 300°C for several days before each set of measurements. The remainder of the vacuum system was carefully outgassed by frequent heating with a Bunsen flame. With the cavity, ionization guage, and liquid nitrogen trap isolated from the pumps, an equilibrium pressure of 1 to 5×10^{-7} mm. of mercury could be obtained for several hours. A single series of breakdown measurements takes about this time.

When the equilibrium vacuum is such that a sufficiently high degree of purity can be obtained, the cavity is filled with hydrogen. The hydrogen is introduced into the system by allowing an iron slug encased in glass to fall on a glass neck which separates a flask containing hydrogen from the remainder of the vacuum system. The iron slug is lifted into position by means of a magnet. A small stopcock has been connected between the cavity and pumps so that a small amount of gas can be removed as desired. The pressure of the hydrogen gas is measured by means of a Macleod guage and is calibrated in millimeters of mercury.

The power incident on the cavity is increased by varying the power divider, while the frequency of the signal is maintained at the resonant frequency of the cavity. At a certain value of power, the transmission crystal current will suddenly fall to a lower value. This change indicates that the gas has broken down, and the maximum crystal current indicates the power required for breakdown. Previous to this, the crystal current and attenuator have been calibrated as a function of the thermistor bridge reading so that the incident power can be determined from the crystal current and attenuator dial setting. However, if the bridge is sufficiently stable so that the zero setting does not drift appreciably with time, the breakdown power can be read directly from the thermistor bridge and the above procedure may be omitted.

The r.m.s. breakdown field is obtained from the following relation (7)

$$E_b = \left(\frac{\bar{P}\,Q_u}{.2695\,\epsilon_0 \pi R^2 L \omega_0}\right)^{1/2} \qquad (16)$$

where P is the power absorbed in the cavity, Q is the unloaded Q of the cavity, and ω_0 is the resonant frequency. The unloaded Q is calculated from the standing wave measurements. The experimental procedure may be found in references (7) and (8). The power absorbed is calculated from the power incident on the cavity and the standing wave ratio of the cavity at resonance. The breakdown field can be measured within an accuracy of approximately 8%. The inherent accuracy of the thermistor bridge is 4 to 5%, and the accuracy in determining the fraction of power to the thermistor bridge is approximately 3%. The pressure can be measured within an accuracy of 1%.

RESULTS

The results obtained in three cavities resonant at 10.6 cm. wave length are shown in Figures 4,5, and 6. The data for the cavity with $L = 10$ cm. was obtained from Karl-Berger Persson. This cavity was excited in the TM_{020}-mode and its resonant frequency was 10.1 cm. The diameters of the other cavities were all the same and equal to that necessary to give a resonant wave length of 10.6 cm. The breakdown field is computed from the measured breakdown power and cavity parameters. Figure 4 shows the experimental breakdown field as a function of pressure for the various cavity lengths. The accuracy of the curves is slightly higher than 15% due to the fact that impurities were present in the hydrogen gas so that the breakdown field was higher. This discrepancy was found by comparing the experimental breakdown fields with those theoretically predicted in reference (9). Further measurements will be performed on the same and additional cavities in order to acquire more accurate results. Every effort will be made to minimize the presence of impurities.

Figure 6, computed from the experimental E versus p curve, depicts the quantity $\left(\frac{1}{E\Lambda}\right)^2$ as a function of E/p for various cavity lengths. If the field were uniform, $\left(\frac{1}{E\Lambda}\right)^2$ would be equal to the high frequency ionization coefficient. However, the non-uniformity must be taken into account, especially for the longer cavities. Figure 5 shows $p\lambda$ plotted as a function E/p. The values of E/p for various $p\lambda$ values may be transferred to Fig. 6 and the constant $p\lambda$ curves are drawn in. The curves are then corrected as described previously to yield a final set of ionization coefficient curves. ζ obtained from these curves is plotted as a function of E_e/p and the assumption that ζ versus E_e/p is a universal curve, being valid in the non-uniform field region, can be verified. These final steps were not performed in this thesis because of the inaccuracy of the present data and the limited time available for the problem. The author, however, intends to continue with the problem until a complete set of data is obtained and the object of this thesis is proved.

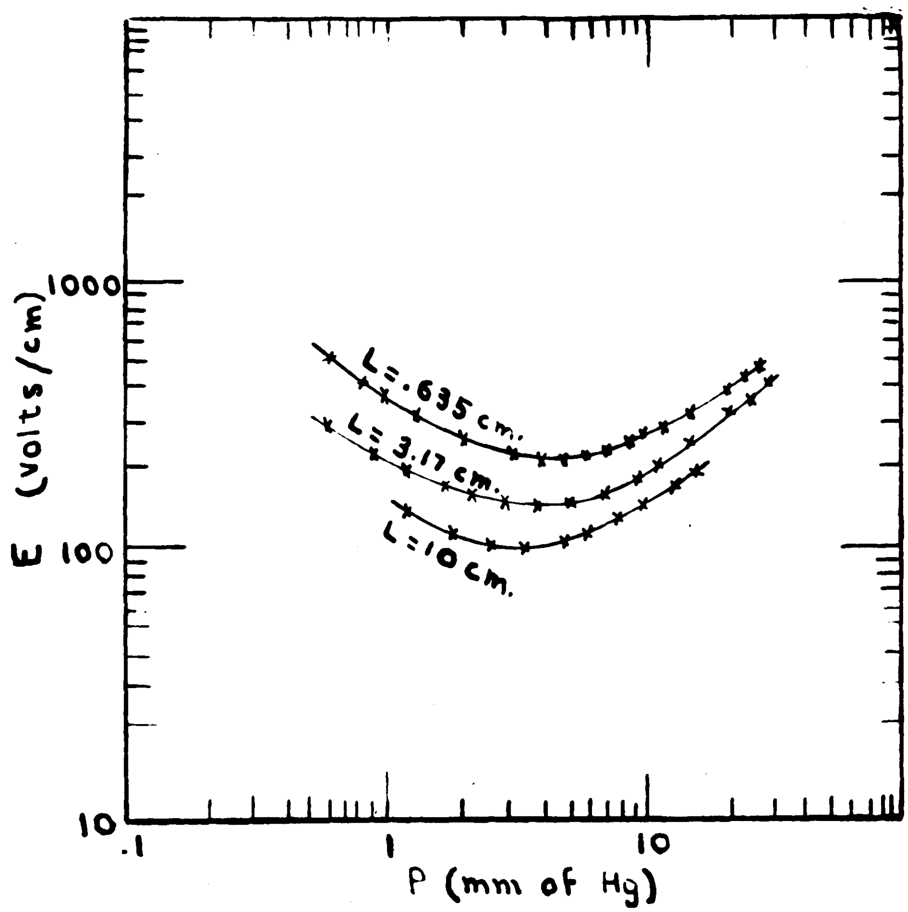

Fig. 4. Experimental values of breakdown field E as a function of pressure p for various cavity lengths.

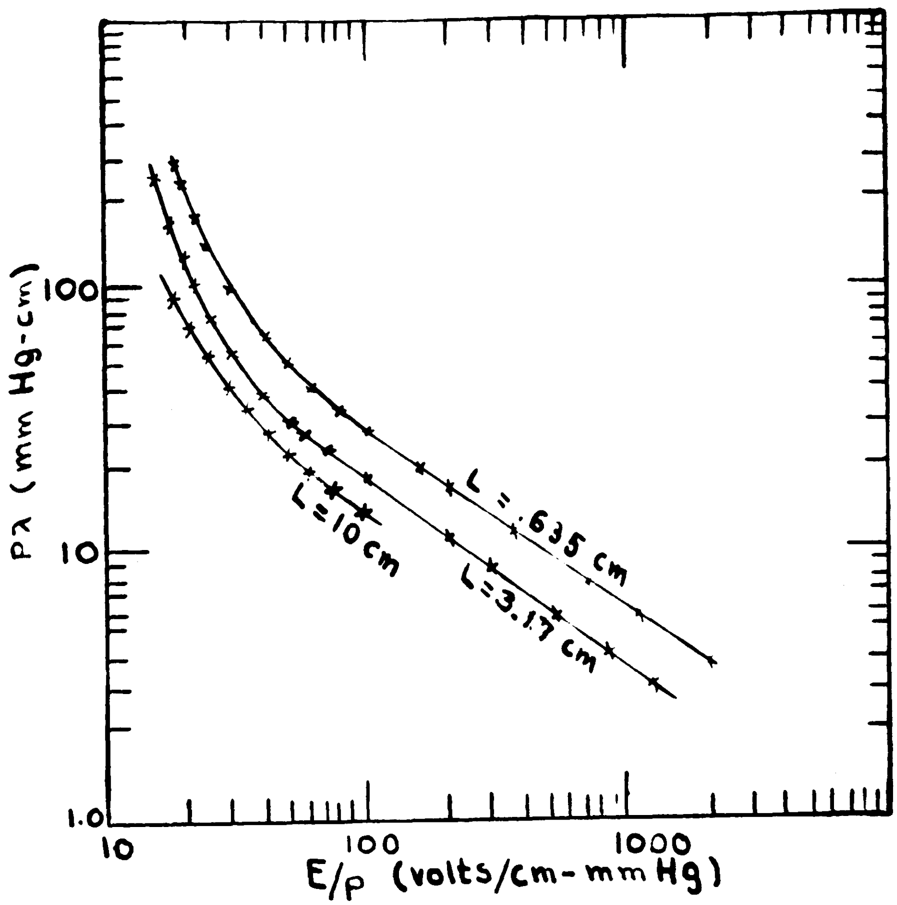

Fig. 5. Curves of pλ versus E/p for various cavity lengths. These curves are used to obtain constant pλ curves in Fig. 6.

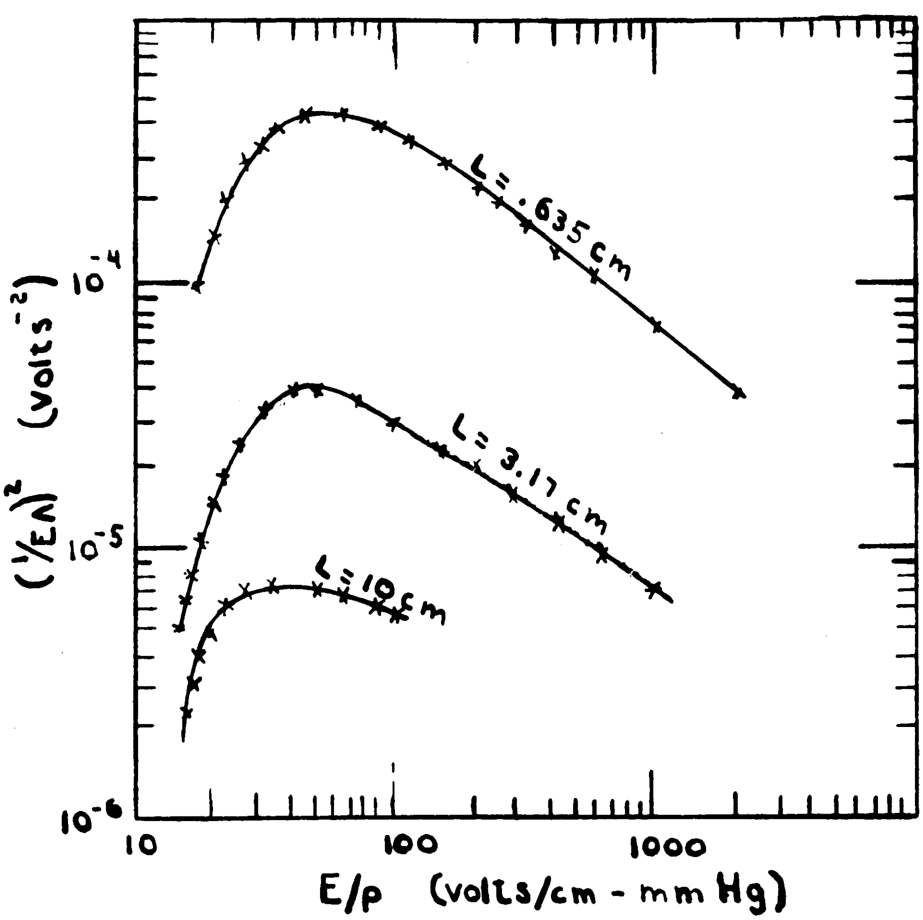

Fig. 6. Experimental values of $\left(\frac{1}{E\Lambda}\right)^2$ as a function of E/p for various cavity lengths, obtained from breakdown field E versus pressure p data. The ordinate would be the high frequency ionization coefficient if the experiment were performed between infinite parallel plates.

REFERENCES

1. M. A. Herlin and S. C. Brown, Phys. Rev. 74,291 (1948).
2. M. A. Herlin and S. C. Brown, Phys. Rev. 74, 910 (1948).
3. W. P. Allis, Lecture Notes, Course 8.232, Physics Department, Massachusetts Institute of Technology (1949).
4. E. Jahnke and F. Emde, <u>Funktionentafeln</u> (B. G. Teubner, Leipzig and Berlin, 1933), p. 275.
5. H. Margenau, Phys. Rev. 69, 508 (1946).
6. A. D. MacDonald and S. C. Brown, Canadian Journal of Research, A, 28, 168 (March, 1950).
7. S. C. Brown, et Al., Methods of Measuring the Properties of Ionized Gases at Microwave Frequencies, Technical Report No. 66, Research Laboratory of Electronics, M. I. T. (1948).
8. C. G. Montgomery, <u>Technique of Microwave Measurements</u>, McGraw-Hill, M. I. T. (1947).
9. A. D. MacDonald and S. C. Brown, Phys. Rev. 76, 1634 (1949).